Supplementary Information

Photostability of CdSe Quantum Dots Under Visible Light Irradiation: Effects of Surface Ligands, Solvents, and BHT Antioxidant

Zijian Wang [a], Shuang Gao [a], Shihao Xu [a], Liang Sun [b], Yudong Liu [b], Jinlong Zhang [a], Baozhu Tian [a] *

[a] State key laboratory of green chemical engineering and industrial catalysis, Shanghai Engineering Research Center for Multi-media Environmental Catalysis and Resource Utilization, Key Laboratory of Specially Functional Polymeric Materials and Related Technology (Ministry of Education), Key Laboratory for Advanced Materials and Joint International Research Laboratory of Precision Chemistry and Molecular Engineering, School of Chemistry and Molecular Engineering, East China University of Science and Technology, 130 Meilong Road, Shanghai 200237, PR China

[b] Research Institute of Physical and Chemical Engineering of Nuclear Industry, 168 JinTang Road, Tianjin, 300180, PR China

* Corresponding author.

E-mail addresses: baozhutian@ecust.edu.cn (B. Tian). Tel：+86 21 64252062

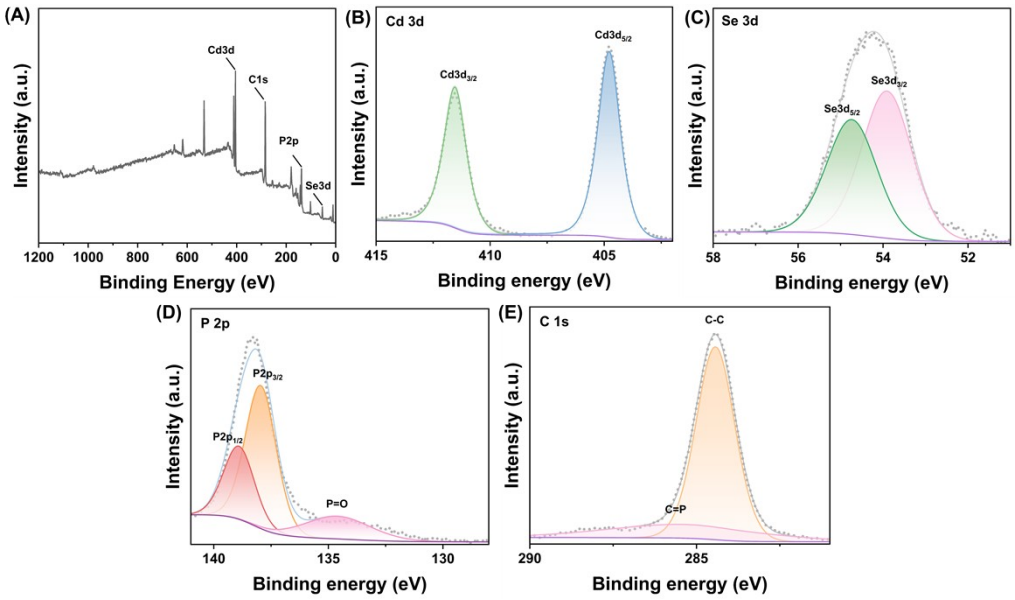

Fig. S1. XPS spectra of CdSe-TBP QDs: (A) Survey spectrum; (B) Cd^{2+} 3d; (C) Se^{2-} 3d; (D) P 2p; (E) C 1s.

Fig. S1A shows the survey spectrum, while Figs. S1B–E display the high-resolution spectra of Cd^{2+} 3d, Se^{2-} 3d, P 2p, and C 1s, respectively. In Fig. S1B, the characteristic peaks at 405.1 eV and 411.9 eV correspond to the Cd^{2+} $3d_{5/2}$ and Cd^{2+} $3d_{3/2}$, respectively [S1]. The Se 3d spectrum in Fig. S1C can be fitted with a doublet located at 53.9 eV and 54.7 eV, corresponding to Se^{2-} $3d_{5/2}$ and Se^{2-} $3d_{3/2}$, respectively [S2]. In Fig. S1D, the two peaks at 138.4 eV and 139.1 eV, is attributed to the P $2p_{1/2}$ and P $2p_{3/2}$ of TBP, respectively. Additionally, due to the facile oxidation of TBP, a shoulder peak near 135.1 eV is observed, which is consistent with the formation of P=O bonds and indicates partial oxidation of the surface phosphine ligands. As shown in Fig. S1E, the peak at 284.8 eV corresponds to alkyl carbon. The signal at 285.7 eV is associated with carbon in C-P bond, confirming the successful surface modification of the QDs with TBP [S3, S4, S5].

References

[S1] G. Granados-Oliveros et al., *J. Mol. Struct.*, 2022. 1254, 132293.

[S2] J.E.B. Katari et al., *J. Phys. Chem.,* 1994. 98, 4109–4117.

[S3] E. Bernes et al., *J. Phys. Chem. C*, 2020. 124, 14510–14520.

[S4] W. Kim et al., *J. Phys. Chem. C*, 2010, 114, 1539–1546.

[S5] Kaneda, G., et al., *Appl. Surf. Sci.*, 1997, 113–114, 546–550.

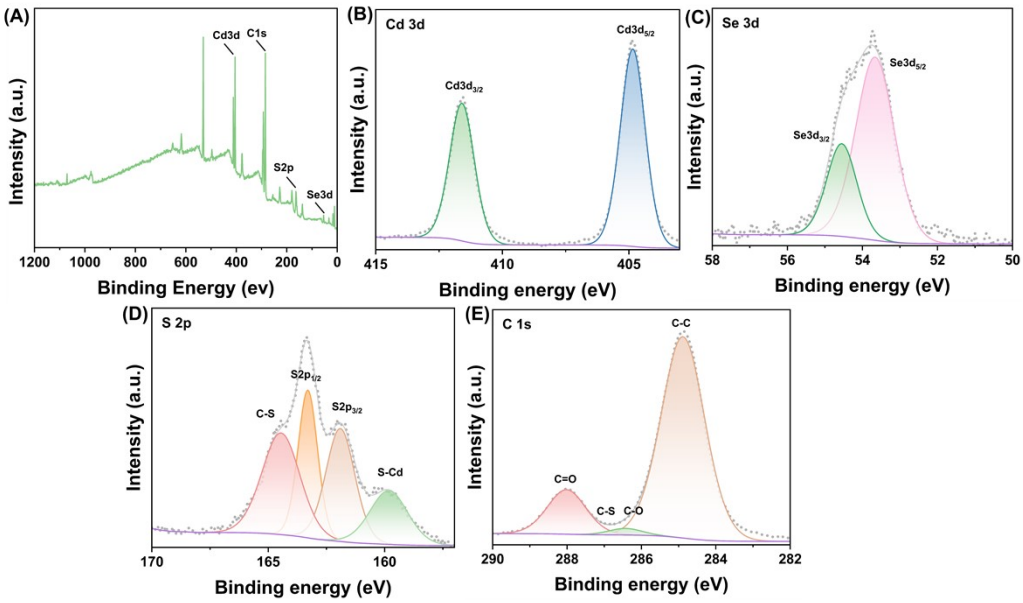

Fig. S2. XPS spectra of CdSe-MPA QDs: (A) Survey spectrum; (B) Cd^{2+} 3d; (C) Se^{2-} 3d; (D) S 2p; (E) C 1s.

To further investigate the elemental composition and chemical structure of CdSe-MPA QDs, XPS characterization was systematically performed as shown in Fig. S2A, with corresponding high-resolution spectra presented in Fig. S2A-S2B. In Fig. S2B, the characteristic peaks observe at 405.1 eV and 411.9 eV correspond to the Cd $3d_{5/2}$ and Cd $3d_{3/2}$ orbitals, respectively [S1]. The Se 3d spectrum in Fig. S2C can be fitted with a doublet, where the peaks locate at 53.8 eV and 54.6 eV correspond to the Se $3d_{5/2}$ and Se $3d_{3/2}$ orbitals [S2]. As shown in Fig. S2D, the doublet at 163.2 eV and 161.8 eV correspond to the S $2p_{3/2}$ and S $2p_{1/2}$ orbitals, respectively. Additionally, a peak at 164.3 eV indicates the presence of C-S bonds, while another peak at 159.7 eV correspond to S-Cd bonds. In the Fig. S2E, peaks are identified at 287.2 eV for C=O bonds, at 286.3 eV for both C-S and C-O bonds, and at 284.8 eV for C-C bonds. These results collectively confirm the successful surface modification of the QDs with MPA [S3, S6, S7].

References

[S1] G. Granados-Oliveros et al., *J. Mol. Struct*., 2022. 1254, 132293.

[S2] J.E.B. Katari et al., *J. Phys. Chem*., 1994. 98, 4109–4117.

[S3] E. Bernes et al., *J. Phys. Chem. C*, 2020. 124, 14510–14520.

[S6] B. Bajorowicz et al., *Appl. Catal. B*., 2017, 203, 452–464.

[S7] A.E. Raevskaya et al., *Nano-Struct. Nano-Objects*, 2018, 13, 146–154.

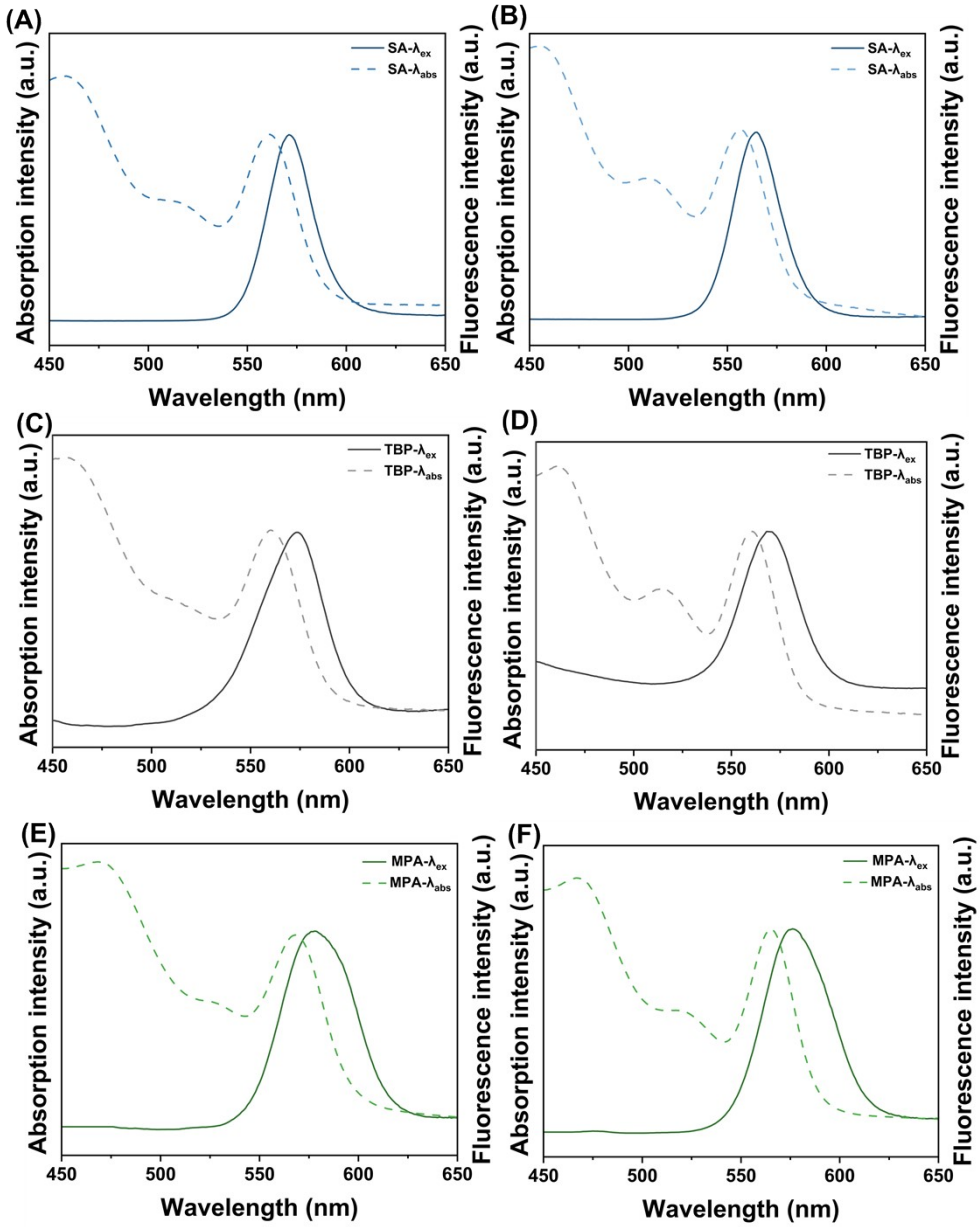

Fig. S3. Absorption and fluorescence emission spectra of (A) CdSe-SA QDs in toluene, (B) CdSe-SA QDs in n-hexane, (C) CdSe-TBP QDs in toluene, (D) CdSe-TBP QDs in n-hexane, (E) CdSe-MPA QDs in ethanol, and (F) CdSe-MPA in QDs water.

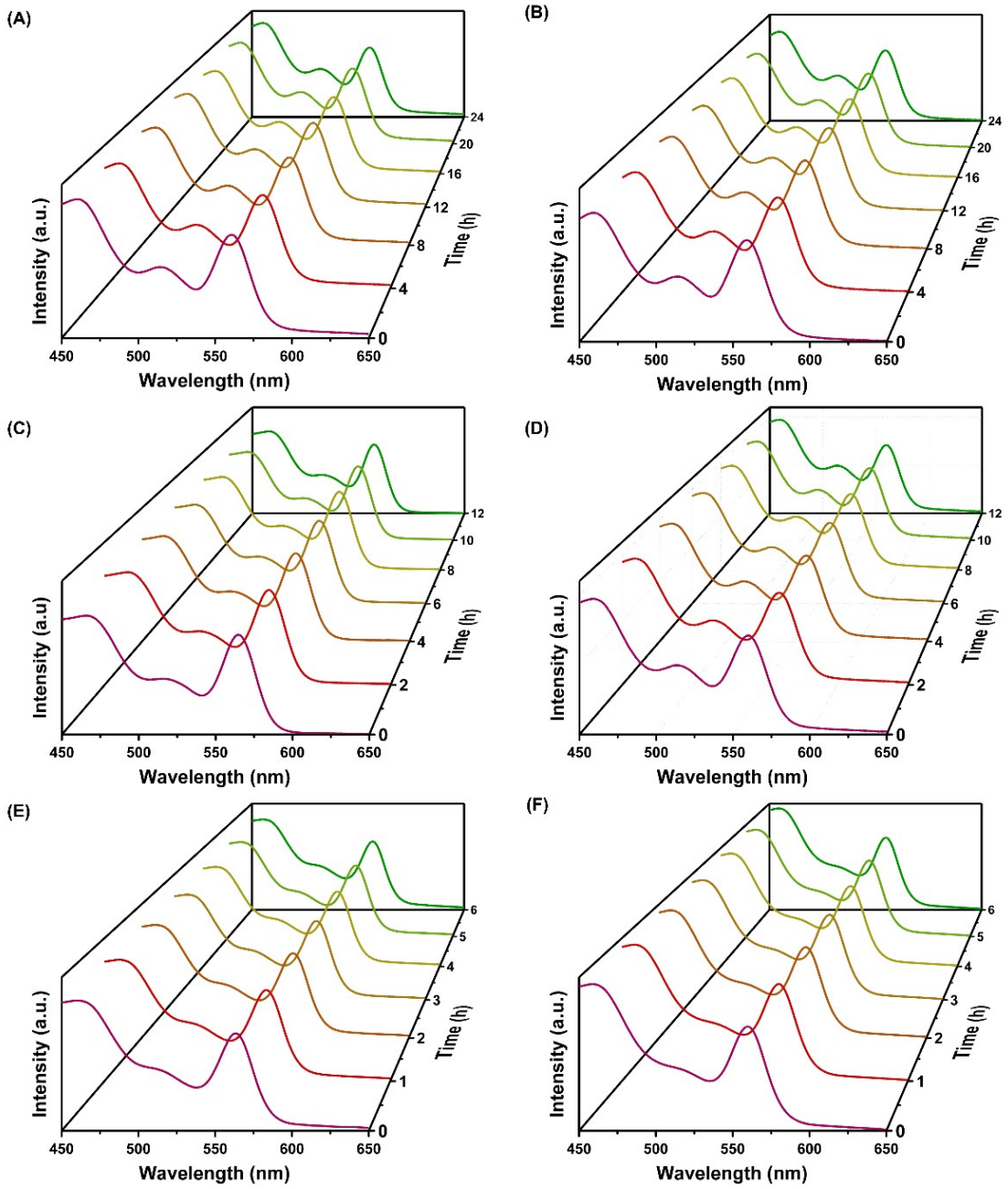

Fig. S4. UV–Vis absorption spectra of different CdSe QDs measured under dark conditions: (A) CdSe-SA QDs in n-hexane; (B) CdSe-SA QDs in toluene; (C) CdSe-TBP QDs in n-hexane; (D) CdSe-SA QDs in toluene; (E) CdSe-MPA QDs in water; (F) CdSe-MPA QDs in ethanol.

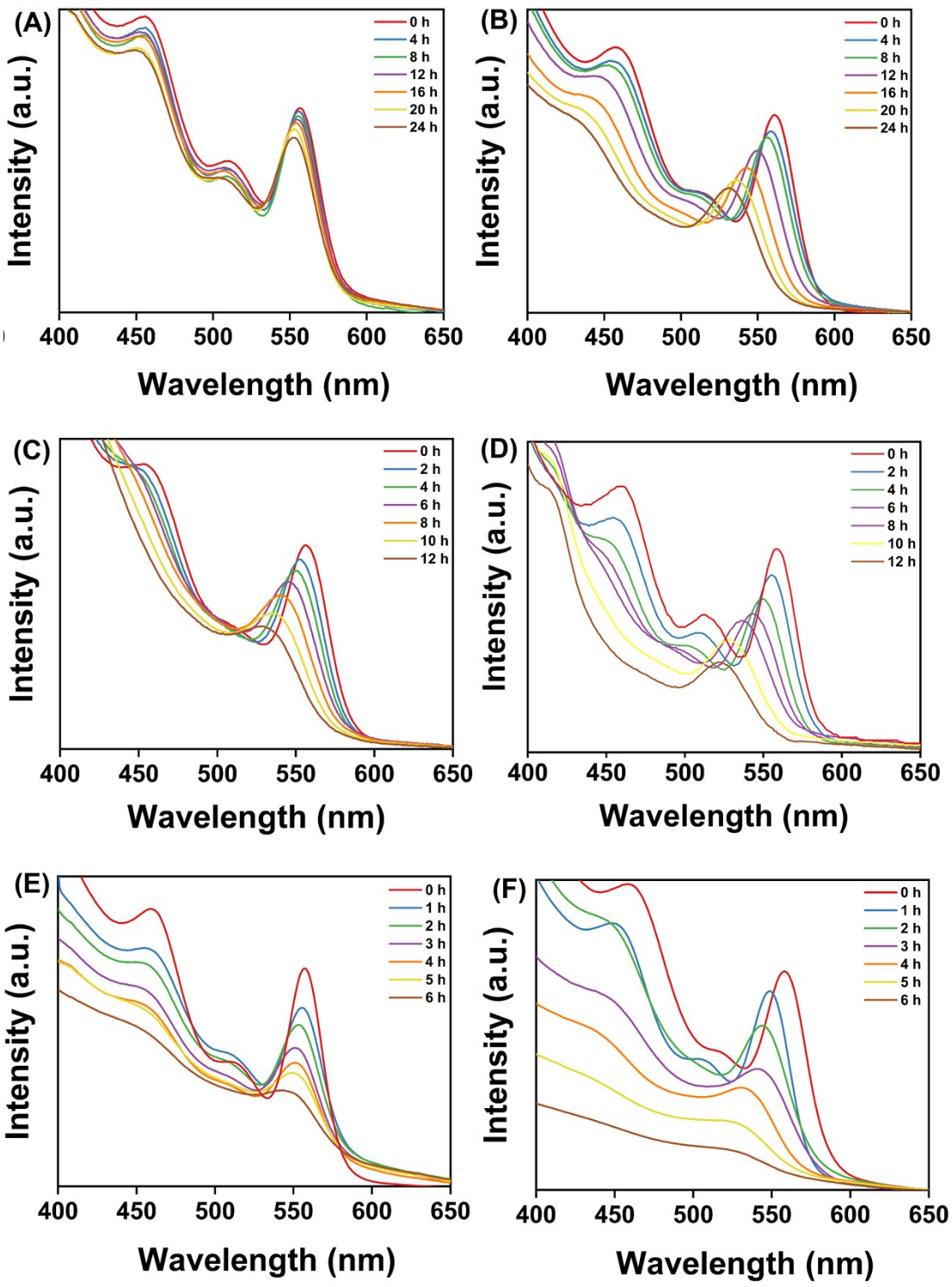

Fig. S5. Time-dependent absorption spectra of CdSe QDs in different O_2-saturated solvents under Xe lamp irradiation: (A) CdSe-SA QDs in n-hexane; (B) CdSe-SA QDs in toluene; (C) CdSe-TBP QDs in n-hexane; (D) CdSe-SA QDs in toluene; (E) CdSe-MPA QDs in water; (F) CdSe-MPA QDs in ethanol.

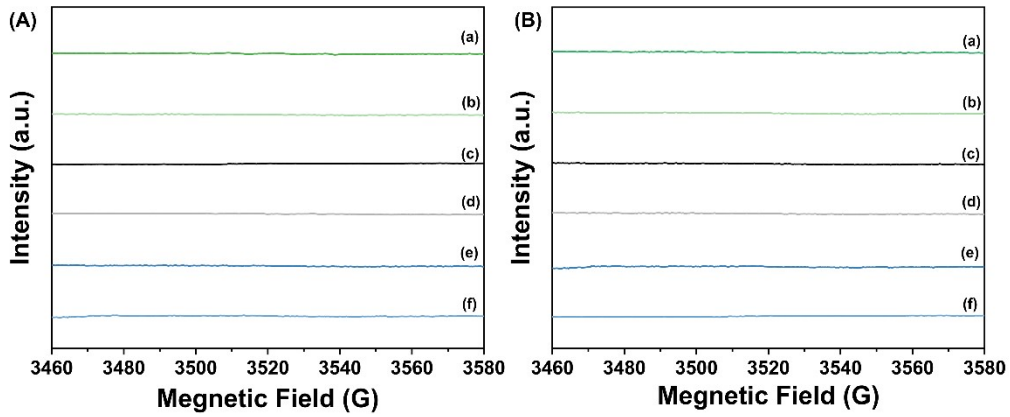

Fig. S6. EPR spectra of $^1O_2$ ($\bullet O_2^-$) in TEMP(DMPO) and different CdSe QDs in the dark: (a) CdSe-MPA QDs in water; (b) CdSe-MPA QDs in ethanol; (c) CdSe-TBP QDs in n-hexane; (d) CdSe-SA QDs in toluene; (e) CdSe-SA QDs in n-hexane; (f) CdSe-SA QDs in toluene.

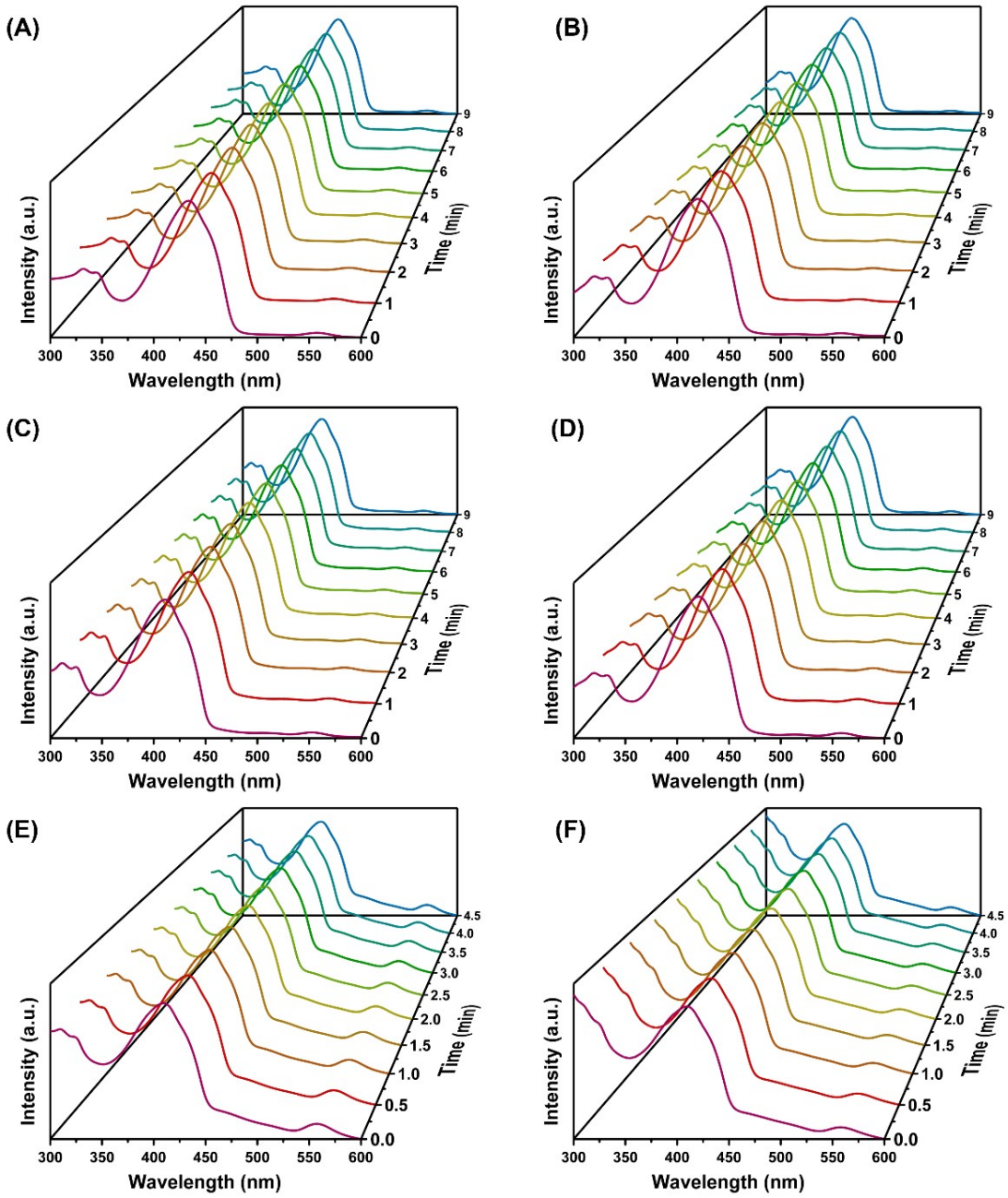

Fig. S7. UV–Vis absorption spectra of CdSe QDs + DPBF measured under dark conditions: (A) CdSe-SA QDs in n-hexane; (B) CdSe-SA QDs in toluene; (C) CdSe-TBP QDs in n-hexane; (D) CdSe-SA QDs in toluene; (E) CdSe-MPA QDs in water; (F) CdSe-MPA QDs in ethanol.

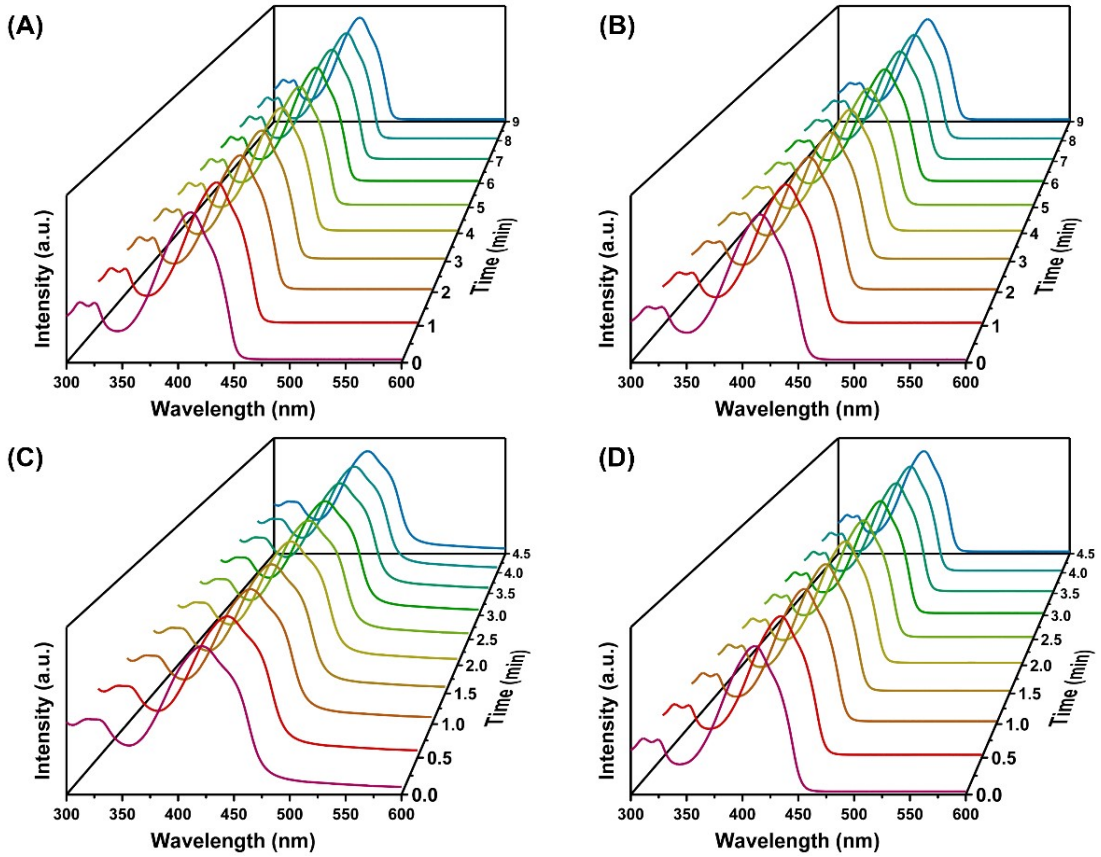

Fig. S8. UV–Vis absorption spectra of DPBF measured in different solvents under light irradiation in the absence of CdSe QDs: (A) n-hexane; (B) toluene; (C) water; (D) ethanol.

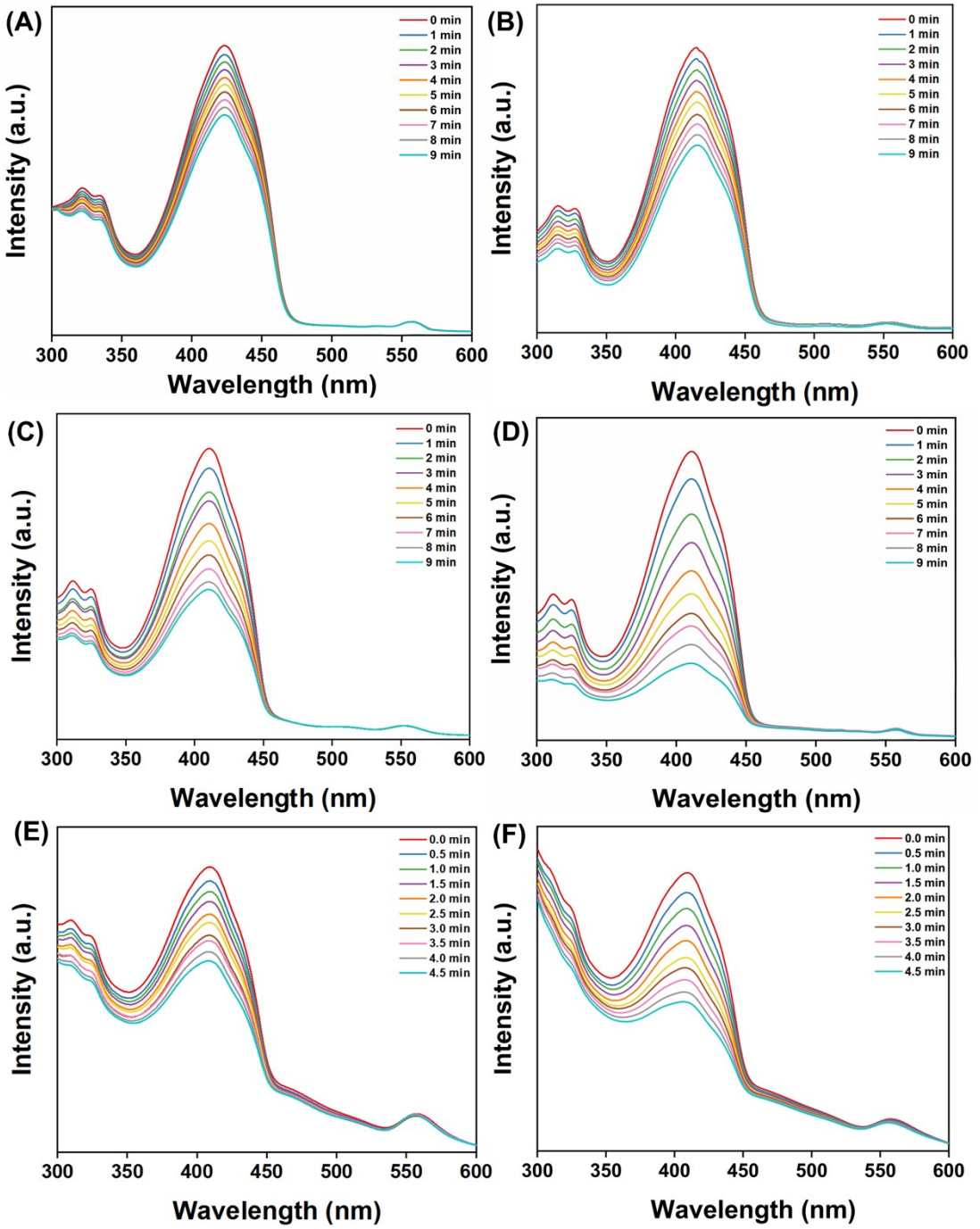

Fig. S9. Time-dependent absorption spectra of CdSe QDs solutions containing DPBF under Xe lamp irradiation: (A) CdSe-SA QDs in n-hexane; (B) CdSe-SA QDs in toluene; (C) CdSe-TBP QDs in n-hexane; (D) CdSe-SA QDs in toluene; (E) CdSe-MPA QDs in water; (F) CdSe-MPA QDs in ethanol.